Journal of Newviews in Engineering and Technology (JNET)
Vol 4, Issue 2, August 2022
Available online at http://www.rsujnet.org/index.php/publications/2022-edition
e- ISSN: 2795-2215

Effect of the Regenerator on Li-ion and Lead Deep Cells

Amadi, Rex Kemkom Chima, Ideriah, Felix J. K., Sodiki, John I. and Nkoi, Barinyima
Department of Mechanical Engineering, Faculty of Engineering, Rivers State University, Nkpolu Oroworukwo, Nigeria.
kemkom.amadi1@ust.edu.ng, +234(0)8036696788

ABSTRACT

This research work posits the ability of Lithium-ion (Li-ion) battery to adapt to other features in the energy recycling terrain in the presence of a suitable thermal source for radiation release. This ability was also compared to that from lead acid battery. It involved the use of experimentation to recycle the energy in the deep cells. The deep cells battery was connected through the inverter to the thermal source (the regenerator) by means of suitable cable leads. The thermal source was linked to a photovoltaic (PV) panel by radiation release. This PV panel then harnessed the radiant energy and converts it to electric energy which is controlled by the charge controller and to the battery. The experiment was conducted with Li-ion deep cells and results of voltage taken from the battery terminal. The Li-ion deep cells battery was replaced with lead acid deep cells battery and results also recorded. The recorded results showed an increase in voltage from 12.54 V to 12.84 V in 12hrs at 300w regenerator radiation level while for the lead acid, there was a voltage reduction. It was established that the pyrophosphate technology inherent in Li-ion made it possible for chargeability to occur despite the energy loss along the chain. The presence of Lead tetra-oxo sulphate (VI) in the lead acid system impeded the progress in the charging process.

KEYWORDS: Regenerator, Pyrophosphate, Li-ion, Deep cells, Lead acid

Cite This Paper: Amadi, R. K. C., Ideriah, F. J. K., Sodiki, J. I. & Nkoi, B. (2022). Effect of the Regenerator on Li-ion and Lead Deep Cells. *Journal of Newviews in Engineering and Technology*. 4(2), 1 – 9.

1. INTRODUCTION

As technology evolves from the use of the very environmentally unfriendly fossil fuel to the introduction of the exceptionally clean solar energy, sustainability of the surplus-existing radiant sourced energy is rapidly gaining grounds. As such, varying technological approaches are being adopted to properly posit this area of renewable energy development and usage. Solar energy is usually harnessed using solar cells, controlled using solar charge controllers (Wali *et al.*, 2022; Amadi & Leol, 2018; Akiza *et al.*, 2021). They may be used directly in DC supplies in which case storage is not required or may be used indirectly by being stored in deep cells and utilized when required for whatever requisite reasons though, would require an extra component - the inverter to become an alternating current (Kan, 2003; Ando *et al.*, 2018).

This study is necessitated by the inherent ability of two groups of solar deep cells, the Li-ion, and the lead acid groups of solar deep cells. The study involves the experimental determination of the charge-ability potential of both deep cell group under controlled environment. It also involves the study of their discharge potentials. Further studies were conducted in the presence of a special component, the regenerator- and the ability of both batteries observed. Lead acid is known to have an inherent poor dynamic charge acceptance with high irreversible sulphation and dendritic deposition which further reduces the state of charge (Moseley *et al.*, 2015; Calborean *et al.*, 2020; Sugumaran *et al.*, 2021).

This work is aimed at determining the effect of the regenerator on Li-ion and Lead deep cells. The specific objectives pursued were to:

i. Evaluate the recharging potential of Li-ion battery
ii. Evaluate the recharging potential of Lead acid battery
iii. Evaluate the energy flow for the system.

Deep cells are known to store energy that is required for consumption and released when processing. Studies are yet to show the effect of

Journal of Newviews in Engineering and Technology (JNET)
Vol 4, Issue 2, August 2022
Available online at http://www.rsujnet.org/index.php/publications/2022-edition
e- ISSN: 2795-2215

re-insolating the deep cell energy to recharge the same deep cell. This work attempts to use the technology behind the production of some of the deep cells with the help of an efficient regenerator to demonstrate this effect.

2. MATERIALS AND METHODS

This section describes the under-laying theories and formulations requisite for the work.

2.1 Lead Acid Deep Cell Theory

Led acid deep cells operate with two electrodes. The deep cell is provided with a negatively charged lead (Pb) electrode and a positively charged Lead dioxide (PbO_2) electrode immersed in Sulphuric Acid (H_2SO_4). Energy storage is a function of the potential difference between these two electrodes. The charging and discharge processes occur because of an interplay between the formation and disintegration of water molecules. Hence, charging occurs with the splitting of water molecules into its constituent ions (i.e., H^+ and O^{2-}). The reverse occurs during the discharge process. The general reaction is denoted in Equation (1).

$$\mathrm{Pb(s) + PbO_2(s) + 2H_2SO_4(aq) \rightarrow 2PbSO_4(s) + 2H_2O\,(l)} \quad (1)$$

Further acceptance of charge is affected by this sulphation and as such does not allow for ultra-fast charging (Pavlov, 2011).

2.2 Solar Lithium-Deep Cell Theory

Solar Li-ion deep cells (batteries) operate based on electrochemical reactions to store energy. The lithium battery transfer charges between lithium cathode and carbon anode divided by a separator. The first few cycles charging and discharging and forms a solid electricity interface which blocks electron flow but permits Li^+ conduction, which further limits electrolyte decomposition. It then utilizes the pyrophosphate technology to attain a proper state of charge through its reversible ultrafast charging technique. This also augments for losses in the regeneration system (Amadi *et al.*, 2019).

2.2.1 Pyrophosphate Technology

$LiFePO_4$ absorbs and releases energy by simultaneous extraction and insertion of Lithium ions and electrons. The battery power depends on the rate of migration of Li^+ and e^- through the electrolyte and the composite structure of the electrode material. The low-rate performance could be improved by improving electron transfer in the bulk at the surface of material and by the reduction of the path length of Li^+ or e^+ by using nanomaterials. Li^+ exchanges electrons with all surfaces and goes into the bulk in the [010] crystal direction increasing diffusion across the [010] facet. This enhances the rate capability of pyrophosphate (Zhu *et al.*, 2013).

LiFePO4 attains ultrafast charging because its structure allows diffusion in the (010) facet (plane) which improves diffusion as the e^- replace the Li^+ and hence allowing an ultra-high charging (Kang & Cedar, 2009; Zhu *et al.*, 2013; Wood *et al.*, 2018). The state of charge of the deep cell has been mathematically narrowed down to depict the difference between the power absorbed by the solar panel and the power taken by the recharger unit as shown by battery dynamics.

2.2.2 Battery Dynamics

According to Kang and Cedar (2013), the state of charge at a particular time (SOC_k) has a relationship with the initial state of charge (SOC_0) and the battery efficiency (η_B) , maximum capacity (E^{max}) and the difference between discharge and recharge values (P_3) is given as:

$$SOC_K = SOC_0 - \propto P_{3k} \quad (2)$$

State of charge at the next time of charge (SOC_{K+1}), where k is an interger for the kth time interval, depends on the available SOC, SOC(k)

$$SOC_{K+1} = SOC_K - \propto P_{3k} \quad (3)$$

where

$$\text{Battery coefficient } (\propto) = \frac{\eta_B}{E}\Delta\tau \quad (4)$$

$\Delta\tau$ is the time interval while E is the battery capacity.

Journal of Newviews in Engineering and Technology (JNET)
Vol 4, Issue 2, August 2022
Available online at http://www.rsujnet.org/index.php/publications/2022-edition
e- ISSN: 2795-2215

For solar deep cell with pyrophosphate technology, Kang and Cedar (2009) implied that:

$$\propto P_{(3)} = \propto_2 p_{discharge-} \propto_1 P_{recharge} \quad (5)$$

here battery coefficient at recharge ($\propto_1$) and battery coefficient at discharge ($\propto_2$) are

$$\propto_1 = \frac{\eta_{B_{recharge}}}{E^{max}} \Delta\tau \quad (6)$$

$$\propto_2 = \frac{\eta_{B_{discharge}}}{E^{max}} \Delta\tau \quad (7)$$

and

$$\eta_{B_{recharge}} = \frac{recharge\ rate\ (\%)}{storage} \quad (8)$$

$$\eta_{B_{discharge}} = \frac{dicharge\ rate\ (\%)}{storage} \quad (9)$$

hence, at the next charge,

$$SOC_{(k+1)} = SOC_{(k)} - \left(P\eta_{B_{discharge}} - P\eta_{B_{recharge}}\right) \quad (10)$$

Power Balance

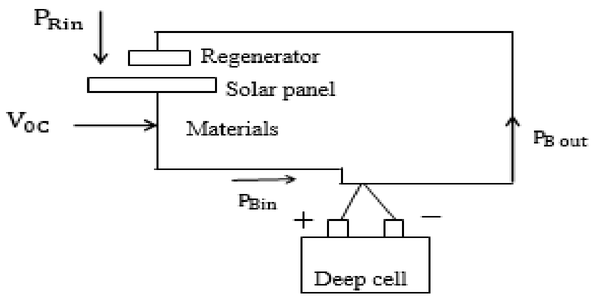

Figure 1: Schematic of Regenerator Set – up

Battery Power

The input power to the battery $\left(P_{B_{in}}\right)$ is the sum of the storage $\left(P_{B_{accm}}\right)$ and the output to the battery $\left(P_{B_{out}}\right)$

i.e.

$$P_{B_{in}} = P_{B_{accm}} + P_{B_{out}} \quad (11)$$

The battery power output is equal to the regenerator power input $P_{R_{in}}$ and the power absorbed by PV (P_{abs}) is equal to the battery power input as

$$P_{B_{out}} = P_{R_{in}} \quad (12)$$

and

$$P_{abs} = IV_{ocv} = P_{B_{in}} \quad (13)$$

Substitute Equation. (13) into Equation. (11)

$$P_{abs} = P_{B_{accm}} + P_{B_{out}} \quad (14)$$

Let, $P_{B_{accm}}$ be the state of charge

then,

$$P_{abs} = SOC_{k+1} + P_{R_{in}} \quad (15)$$

The state of charge depends on the pyrophosphate technology available and as such augments the power balance required especially when the regenerator does minimise power loss.

2.2.3 Solar Deep Cells Principle behind the Application of a Regenerator to Recharge the Deep Cell

The solar deep cell contains area of electrolytic charging and discharging at the battery anode and cathode with $Li\,Fe\,PO_4$ materials that provides the charging, holding and discharge surfaces. Pyrophosphate materials are applied to provide an ultra-charging condition. Increase in the holding time of the deep cell can also be achieved using fine crystal coatings rather than coarse coating on the storage material since it allows or permits only a slow discharge (Kang & Cedar 2009). Factors that support the application of the regenerator in the current work are

i. Utilization of a regenerator with high reflectivity.
ii. Utilization of a deep cell with ultra-high charging
iii. Utilization of a deep cell with a slow discharging rate.

This simply implies that the level of doping at the electrodes can determine how fast a charging operation can occur and how slow a discharge operation occurs. The highly reflective regenerator takes in energy from the battery and releases a great amount of the energy, which re-enters the battery through PV cells and recharge the same battery due to the pyrophosphate ultra-charging situation. The regenerator can take energy from the deep cell and recharge that same deep cell because of the following:

The state of charge at a particular time (SOC_k) has a relationship with the initial state of charge (SOC_0) and the battery efficiency(η_B),

Journal of Newviews in Engineering and Technology (JNET)
Vol 4, Issue 2, August 2022
Available online at http://www.rsujnet.org/index.php/publications/2022-edition
e- ISSN: 2795-2215

maximum capacity (E^{max}) and the difference between discharge and recharge values.

2.2.4 Determination of recharging, rechargeability, and charging rate.

The Determination of recharging, rechargeability, and charging rate were based on the state of charge of the deep cells. This is measured with the voltmeter in voltages at various levels of charge. In this study, the experimental rig used to demonstrate and obtain the required data comprised of the PV cell with cable leads, charge controller, Li-ion battery, 8mm wires and inverter, recharger, voltmeter, and timer. These materials were connected as shown in Figure 2. With some stored energy in the battery, power flows through the inverter to the recharger. The recharger then releases radiation which is converted to electricity at the PV panel and further regulated by the charge controller before reaching the battery.

The experiment was used to determine the occurrence of battery recharging, panel voltages at which battery rechargeability could occur, recharge rate at specific recharge power and monitoring recharge under external load only. The Li-ion battery was replaced with a lead acid deep cells battery to determine and compare the batteries characteristics. Voltage drop and the time taken per voltage drop were recorded. The experiment was repeated with the recharger removed from the charging position (i.e., from the top of the panel) and, used as external load. Results were also recorded.

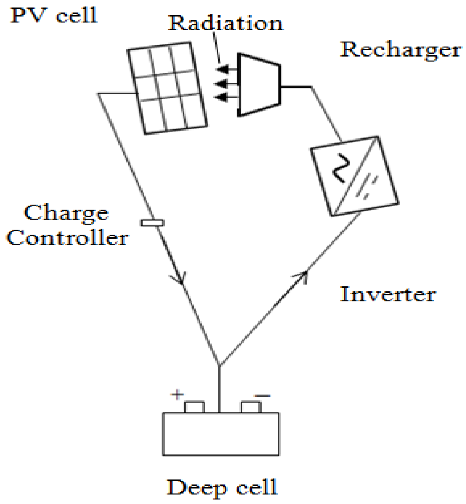

Figure 2: Schematic Diagram of Experimental Set – up

3. RESULTS AND DISCUSSION

3.1 Battery Recharging Process

The result of the ability of the regenerator to recharge the Lithium-ion deep cells over a duration of twelve hours is shown in Figure 3.

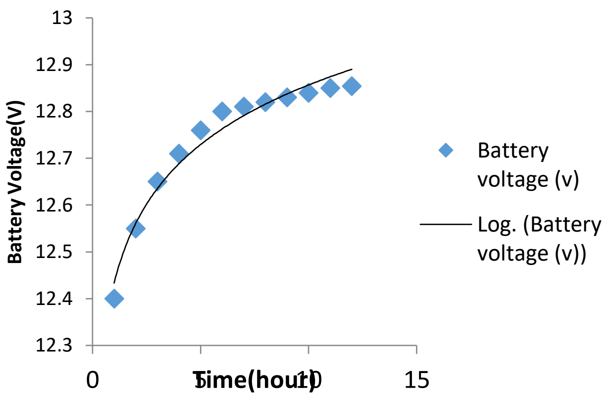

Figure 3: Li-ion Recharge at 300 W Constant Power Input Over the Hour Time Duration

Figure 3 depicts the variation of battery voltage over 12-hour duration of the day under recharge. The trend shows that at a constant power input of 300W from the incandescent – sourced – cascade to the photovoltaic panel, an overall ascendancy occurred as the output voltage increased with time. The steepness of the curve up to the sixth (6^{th}) hour is indicative of a fast rate of charge while the trend flattened out towards the twelfth (12^{th}) hour. This is because

Journal of Newviews in Engineering and Technology (JNET)
Vol 4, Issue 2, August 2022
Available online at http://www.rsujnet.org/index.php/publications/2022-edition
e- ISSN: 2795-2215

charging the deep cell occurs at a faster rate at low storage capacity and at a slower rate at high storage capacity.

Also, this situation relates to cell temperature build up with increased voltage during recharging that also increases the resistance to further charging, hence the gradually reducing slope of the curve at high battery voltage. The observed trend agrees with that from the studies of Zhu *et al*. (2019) which provided that the battery charges faster up to 60%, followed by 30% of the battery. The remaining 10% of the battery is charged slowly (trickle charging). Figure 5 agrees with the graph of Buchmann 2019 in Figure 4. Figure 4 was used to validate Figure 3 and shows how deep cells recharge.

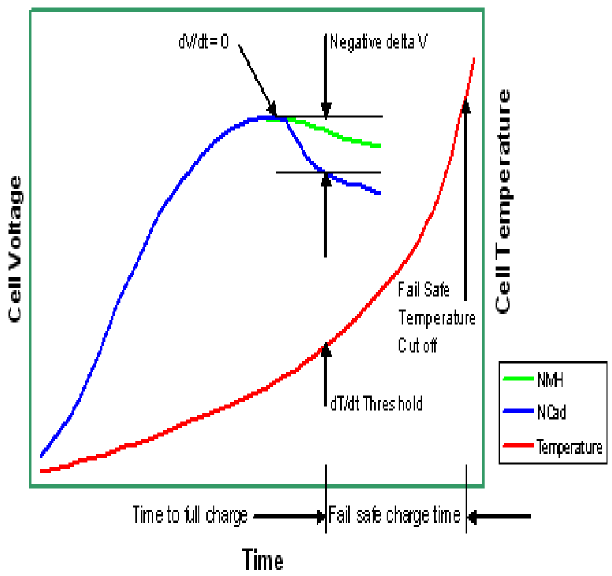

Figure 4: Buchmann 2019's Charge Characteristics for Cell Voltage vs Time

3.2 Recharge/Discharge Behaviour of Lead-Acid Deep Cells Showing Depletion Characteristics

The functionality and performance of a lead-acid deep cells in storing energy while in connection with the recharging component was assessed by observing the recharge and discharge behaviour when it is connected to recharger and consumption unit (no recharger) respectively as is shown in Figure 5.

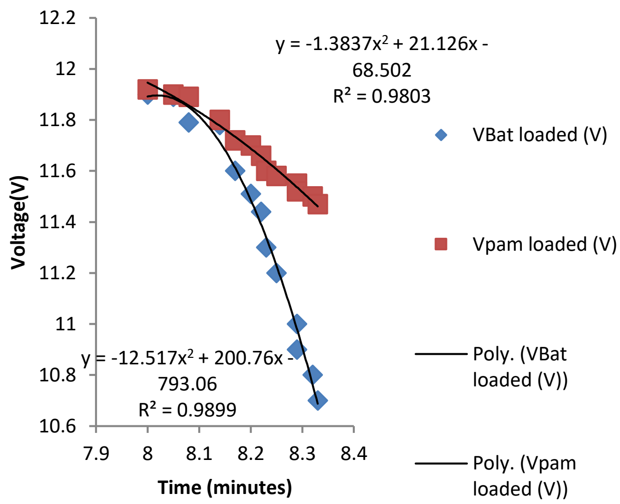

Figure 5: Depleting Deep Cell Characteristics of Lead Acid Deep Cells

This assay was used to show the characteristics of a depleting deep cell under recharge. It presents V_{pan} (loaded) as the panel voltage when the recharger is the only source of radiation without an external load and V_{Bat} (loaded) as the corresponding voltage of the battery. The trend in Figure 5 shows that the depleted deep cell used in the circuit gets discharged with time in 33minutes) rather than being charged. When the same deep cell was discharged of its own, supplying energy to a 25 W output, it took almost same period to be discharged critically (about 27 minutes). The implication is that lead-acid battery does not have a boosting technology to supply extra electrons as was the case of Li-ion battery. The regenerator becomes ineffective and will do no other thing than discharge such deep cells. In other words, when recharge rate becomes less than discharge rate, the entire system discharges the deep cells.

3.3 Limitation of the Work / Critical Fallouts of Experimental Results

The essence of this research is to check the workability of artificial lighting system whose effect is easily noticeable on small solar cells

Journal of Newviews in Engineering and Technology (JNET)
Vol 4, Issue 2, August 2022
Available online at http://www.rsujnet.org/index.php/publications/2022-edition
e- ISSN: 2795-2215

like the type used in calculators. Re-routing the already generated energy/power through an incandescent source to serve as an artificial lighting source, which consequently powers a solar panel in cyclical order portends walking up a potential gradient and a major limitation to the commercial application of this work. This is because of the numerous losses that would be encountered in the process. These losses make it difficult to return sufficient power and energy to efficiently recharge the batteries if the cycle is repeated as is illustrated in Table 3.

Table 3: Energy Estimation for Set-up

Power Input (P_i) (W)	Incident Power ($0.92P_i$) (W)	PV Power Output (P_{out} =W) (W)	Total PV Loss (W)	Battery Input Power (PV Power Output)	Battery Output Power (Regenerator Power P_i)	Battery Accumulation
60	55.2	29.925	25.275	29.925	60	30.75
120	110	97.47	12.53	97.47	120	29
180	165.6	119.07	46.53	119.07	180	61
240	220.3	132.6	87.7	132.6	240	107.4
300	276	167.7	108.3	167.7	300	132.3

These losses are PV losses, battery losses, charge controller losses, inverter losses, cable losses and recharger cascade losses. Charge controller losses, inverter losses and cable losses were assumed as negligible hence not considered in Table 3. Experimental results showed that for an initial insolation with a 60W incandescent source at the regenerator cascade, an insolation value of (55.2/ 0.99) = 55.7W/m^2 was achieved resulting from 8% loss at the regenerator. The question is, would the incandescent source take in the same amount of power/ energy on re-insolation?

Thus, a -55.7W power incident on the PV panel would have the following losses occurring, neglecting charge controller and cable losses as shown:

i. **PV Power Losses (P_L)**: 75% and 72.84% losses mean 25% and 27.16% transmission which is 13.9 W and 15.13 W, respectively. This implies that 13.9 W to 15,13 W will be transmitted to the battery. This is so because the PV module losses is a conglomerate of cells and major system losses occur here. The mode of these losses may appear as surface glass and solar film reflection losses ($P_{opt\ L}$) comprises reflection and absorption losses, thermalization losses from high energy photons ($Q_{th\ L}$), sub-band gap losses from low energy photons ($Q_{sbg\ L}$), resistance losses from transportation path ($Q_{R\ L}$), recombination/emission losses ($P_{em\ L}$) a reflection plus resistance at cell interconnection/ arrangement losses ($Q_{arr\ L}$) (Shen *et al.*, 2020). Hence, the incident radiation (P_{in}) is distributed as

$$P_{in} = Q_T + P_{opt\ L} + P_{em\ L} + P_{space}L + P_{out} \quad (16)$$

where

$$Q_T = Q_{sbg\ L} + Q_{th} + Q_{arr} + Q_R \quad (17)$$

and $P_{space\,L}$ is losses due to space above panel. Also, power loss is

$$P_L = P_{in}(1 - \eta_{PV}) \quad (18)$$

where η_{PV} is PV efficiency. These PV losses are a major reason commercial PV panel efficiency are lower than that of Shockley- Quessier limit which gives efficiency as 30%. This means that the available power for battery recharge is 27.84% of input power (Shen, 2020). World Economic Forum (2017) in Sodiki (2021) placed the power output from PV panel due to losses as being in the order of 25% of the input power

Journal of Newviews in Engineering and Technology (JNET)
Vol 4, Issue 2, August 2022
Available online at http://www.rsujnet.org/index.php/publications/2022-edition
e- ISSN: 2795-2215

ii. **Battery Efficiency Losses**: 20% and 6% losses mean 80% and 94% transmission which is 11.12W to 14.1W, respectively. The implication is that the inverter receives between 11.12W to 14.1W. This is so because losses in battery efficiency is a function of the battery cells, the cell interconnection at a particular state of charge and heat generated. Indeed, the cells develop internal resistance that culminate into temperature rise and losses. Electrical contact resistance losses (R_L) and power loss in Li-ion batteries can range from 6-20% depending on the correctness of the joint connections and the associated surface treatment and approximates as the total measured resistance and corresponds to the voltage drop (ΔV_e) given as

$$R_L = \frac{\Delta V_e}{I} \quad (19)$$

Where I = current

The power (P_L) also known as ohmic loss is generated at the electrode-connector interface and appear as heat generation loss because of electrochemical activities (Taheri *et al.*, 2011). Sodiki (2021) placed battery power loss at 20% given by

$$P_L = I^2 R_L \quad (20)$$

iii. **Inverter Losses**: 10.0W and 2.6% losses means 90% and 97.4% transmission which is 10.0W and 13.73W, respectively. This also shows that 10.0W to 13.73W is transmitted to excite the incandescent source.
Inverters lose power due to conduction and switching losses which occur at diodes and insulate gate bipolar transistors (IGBT) which are usually minimal if compared to the entire losses in the system. These losses are placed at 2.6 – 6.8% (Wei *et al.*, 2017). Nafeh (2009) in Sodiki (2021) placed the losses in the region of 10%.

iv. **Cable Losses:** Losses in cables are extremely low as such could be

v. neglected in line with Sodiki (2021). Though, these losses occur according to the area of cross section of the wires as 1.7% for 15 mm^2, 0.6% for 4 mm^2 and 0.2% for 10 mm^2 (Ekici & Kopru, 2017).

vi. **Charge controller losses:** The charge controllers utilize an algorithm in its operation. They have losses in the range of 1.3-1.8% under standard testing condition (Akiza *et al.*, 2021).

According to Sodiki (2021), re-insolation of that energy on a panel would not generate up to another maximum power equal to 25% of that coming from the battery. The re-insolation value was seen to be less than 18% because of battery efficiency and inverter efficiency.

This finding stands out on critical analysis of batteries. The findings are in consonance with Figure 5 of this work. Figure 5 describes the depleting deep cell characteristics of a lead-acid battery without a boosting technology. As such, the graphical trend showed a reduction with re-insolation.

However, given a battery (Li-ion battery) with a boosting technology like the pyrophosphate technology and its ionization capability inherent in Iron (Fe), experimental result showed an increment in battery recharge voltage state on re-insolation as shown on Figure 3. Though the incremental voltage has its limit known as limit of intercalation of Lithium. At this limit, high lithium removal and high degree of oxidation occurs, and the system may become intrinsically unstable under extreme conditions of use (Whittingham, 2014). This limit is yet to be determined in the current work This forms a major limitation to the work as sustenance of the system on pyrophosphate technology alone could be limited with time, hence not commercially practicable but, of immense academic application.

4. CONCLUSIONS

The effect of the recharger when tested on two distinct types of battery, lithium ion and

Journal of Newviews in Engineering and Technology (JNET)
Vol 4, Issue 2, August 2022
Available online at http://www.rsujnet.org/index.php/publications/2022-edition
e- ISSN: 2795-2215

lead-acid deep cells battery, gave a unique outcome. The lithium-ion produced a positive sloping graph which depicts an increment of charge. On the other hand, the lead-acid battery had a negative sloping trend because of discharge. This clearly shows that the type of battery in use is a requisite factor in attaining recharge. Li-ion battery recharged because of the presence of pyrophosphate which is a boosting technology.

The contribution of this work is that: at 300W regenerator radiation intensity, the voltage increases from 12.54V to 12.84V in 12hrs, while for the lead acid, there was a voltage reduction. As such, some deep cells like Li-ion have the battery to recharge itself, others like lead acid do not have rechargeability potential as shown by this study.

5. ACKNOWLEDGEMENTS

The authors would like to acknowledge the efforts of Prof. M. E. Ephraim, Prof. B. T. Lebele-Alawa, Mr. Orokor Allwell Chiyonu, Mr. Amaechi Chukwuemeka Christian, Mr. Awaji Ubolom Anthony, Mr. Chimaroge Obuah and Mr. Mojana Alexander Owor for their technical support.

REFERENCES

Akiza, B., Akoro, E., & Douti, D. B. L. (2021). Design and Simulation of an MPPT Charge Controller for a PV Application. *TH Wildau Engineering and Natural Sciences Proceedings*. 2nd *German – West African Conference on Sustainable, Renewable Energy Systems* (SusRES 2021). November 6th, 2021, Kara, Togo, 257-261.

Amadi, R. K. C., Ideriah, F. J. K. & Nkoi, B. (2019). Comparison between Regenerator Model and the Instantaneous Direct Solar Radiation for Port Harcourt. *European Journal of Engineering Research & Science*. 4(5), 76-79.

Amadi, R. K. C. & Leol, A. K. (2018). Determination of the Actual Amount of Insolation Absorbed by a Photovoltaic Panel (125W). *Science Journal of Energy Engineering*. 6(1), 27-30.

Ando, Y., Oku, T., Yasuda, M., Shirahata, Y., Ushijima, K., & Murozono, M. (2018). A Compact SiC Photovoltaic Inverter with Maximum Power Point Tracking Function. *Solar Energy*. *141*, 228-235.

Buchmann, I. (2019). *Improved Battery Performance with Proper Battery Charging*. Ed: Cadex, Richmond, BC.

Calborean, A., Bruj, O., Murariu, T., & Morari, C. (2020). Resonance Frequency Analysis of Lead-Acid Cells: An EIS Approach to Predict the State-of-Health. *Journal of Energy Storage*. *27*, 101-143.

Ekici, S. & Kopru, M. A. (2017). Investigation of PV System Cable Losses. *International Journal of Renewable Energy Research*. 7(2), 807-815.

Kang, B., & Ceder, G. (2009). Battery Materials for Ultrafast Charging and Discharging. *Nature*. 458(7235), 190-193.

Moseley, P. T., Rand, D. A., & Peters, K. (2015). Enhancing the Performance of Lead–Acid Batteries with Carbon–In Pursuit of an Understanding. *Journal of Power Sources*. *295*, 268-274.

Nafeh, A. E. A. (2009). Design and Economic Analysis of a Stand-Alone PV System to Electrify a Remote Area Household in Egypt. *The Open Renewable Energy Journal*. 2(33-37), *33-37*

Pavlov, D. (2011). *Lead-Acid Batteries: Science and Technology*. Elsevier.

Shen, L. Li, Z, & Ma, T. (2020). Analysis of the Power Loss and Quantification of Energy Distribution in PV Module. *Applied Energy*. 260(114333), 1-3.

Sodiki, J. I. (2021). Private Communication: Query on the Ability of Attaining a Positive Self-recharge by Deep Cells through PV Panel. Department of Mechanical Engineering, Rivers State

Journal of Newviews in Engineering and Technology (JNET)
Vol 4, Issue 2, August 2022
Available online at http://www.rsujnet.org/index.php/publications/2022-edition
e- ISSN: 2795-2215

University, Port Harcourt. Unpublished.

Sugumaran, N., Everill, P., Swogger, S. W., & Dubey, D. P. (2015). Lead Acid Battery Performance and Cycle Life Increased Through Addition of Discrete Carbon Nanotubes to Both Electrodes. *Journal of Power Sources*, *279*, 281-293.

Taheri, P. Hsieh, S. & Bahrami, M. (2011). Investigating Electrical Contact Resistance Losses in Lithium-Ion Battery & Assemblies for Hybrid and Electric Vehicles. *Journal & Power Sources.* 196 (15), 6525-6533.

Wali, S. A., Amadi, R. K. C., & Orokor, A. C. (2022). Design Analysis of a Solar Power System for the Faculty of Engineering, Rivers State University. *Global Scientific Journals.* 10(3), 1316-1326.

Wei, Ki, Zhang, C. Gong, X., & Kang, T. (2017). The IGBT Losses Analysis and Calculation of Inverter for Two-Seat Electric Circuit Application. *Energy Procedia* 105(2017), 2623-2628.

Whittingham, M. S. (2014) Ultimate Limit to Intercalation Reaction for Lithium Batteries. *Chemical Reviews*. 114(23), 11414-11443.

Zhu, C., Li, X., Song, L., & Xiang, L. (2013). Development of a Theoretically Based Thermal Model for Lithium-Ion Battery Pack. *Journal of Power Sources*. 223, 155-164.